Electronic Supplementary Information

Eu^{III} and Tb^{III} upconversion intermediated by interparticle energy transfer

in functionalized NaLnF$_4$ nanoparticles

Sergio Fernando Nunes Coelho[1], Airton Germano Bispo-Jr[1], Nagyla Alves de Oliveira[1], Italo Odone Mazali[1],

Fernando Aparecido Sigoli[1]*

[1] Department of Inorganic Chemistry, Institute of Chemistry, University of Campinas, Unicamp, Josué de

Castro Street, Cidade Universitária, Campinas, 13083-970, Brazil.

E-mail: fsigoli@unicamp.br

Table of Contents

Supplementary note S1 - Experimental Procedures

Chemicals

Gadolinium oxide (Gd_2O_3, 99.9%), ytterbium oxide (Yb_2O_3, 99.9%), europium oxide (Eu_2O_3, 99.9%), terbium oxide (Tb_4O_7, 99.9%), thulium oxide (Tm_2O_3, 99.9%), trifluoroacetic acid (tfa, 98%), oleic acid (OA, 90%), oleylamine (OAm, 70%), octadecene (ODE, 90%), acetylacetone (acac), 2-thenoyltrifluoroacetone (tta), and 3,5-dibromebenzoic acid (3,5-bbza) were purchased from Sigma-Aldrich. Ethanol (99%) and cyclohexane were purchased from Synth. Sodium hydroxide was purchased Química Moderna, and hydrochloride acid (HCl, 36,5%) from Merck. All chemicals were used as received.

Nanoparticle Synthesis

β-NaGd$_{0.50}$Yb$_{0.49}$Tm$_{0.01}$F$_4$, β-NaGd$_{0.95}$Eu$_{0.05}$F$_4$, β-NaGd$_{0.85}$Eu$_{0.15}$F$_4$, β-NaGd$_{0.785}$Eu$_{0.215}$F$_4$, β-NaGd$_{0.60}$Eu$_{0.40}$F$_4$, β-NaGd$_{0.635}$Eu$_{0.15}$Tb$_{0.215}$F$_4$, and β-NaGd$_{0.215}$Tb$_{0.215}$F$_4$ nanoparticles were synthesized via the thermal decomposition method of lanthanide trifluoroacetate, Ln(tfa)$_3$, as previously reported by our research group[1].

Briefly, for the nanoparticle syntheses, 1.5 mmol of sodium trifluoroacetate (tfaNa) and 1.5 mmol of the Ln(tfa)$_3$ (following the molar concentration of each doping) were mixed in a three-neck round-bottom flask with 30 mmol of 1-octadecene, 15 mmol of oleic acid, and 15 mmol of oleylamine. The mixture was heated to 100 °C under vacuum and stirred for 30 min. In the next step, argon flux was added to the vial, and the reaction was heated to 310 °C for 20 min., forming the cubic β-NaLnF$_4$ phase. After that, to induce the β-NaLnF$_4$ hexagonal phase formation, excess sodium trifluoroacetate (2.6 mmol), 1-octadecene (20 mmol), and oleic acid (20 mmol) were added in the vial and the temperature was increased to 330 °C for 15 min. The suspension was cooled down to room temperature, followed by the addition of ethanol (120 mL) to precipitate the nanoparticles. Finally, the NPs were separated by centrifugation and washed with ethanol, cyclohexane, water, and ethanol.

The nanoparticles free of oleate on the surface (uncapped-NP) were obtained by acid treatment (HCl, 0.1 mol. L^{-1}) up to pH equal to 1.5, followed by stirring for 24 hours, and liquid extraction with diethyl ether, as described elsewere[2]. We also previously discussed that the washing step does not change the β-NaGdF4 structure or lead to nanoparticle leaching.

Functionalized nanoparticle synthesis

In a two-neck round-bottom flask with 15 mL of deionized water, 100 mg (0.45 mmol) of tta, 500 µL (4.8 mmol) of acac$^-$, or 60 mg (0.21 mmol) of 3,5-bbza$^-$ was deprotonated with a stoichiometric amount of NaOH (1 mol L^{-1}) and heated to 80 °C. The pH was then corrected to 5 with an HCl (0.1 mol L^{-1}) solution. In the sequence, 100 mg of the uncapped nanoparticle was added and the dispersion was kept under magnetic stirring and heating at 80 °C for 12 h. After that, the functionalized nanoparticle was centrifuged, washed three times with ethanol, and dried at 80 °C for 24 h.

Assembly of nanoparticle mixing systems

To collect the upconversion emission spectrum of the nanoparticle mixture (1:1 w/w) and infer the interparticle energy transfer, oleate-caped NaGd$_{0.50}$F$_4$: Yb$_{0.49}$Tm$_{0.01}$ donor particle + bbza$^-$, tta$^-$ or acac-functionalized

acceptor nanoparticles were first dispersed in water and placed on the ultrasound for 30 min. After that, the nanoparticle mixture was dried and the UC measurements were undertaken.

Characterization

PXRD. Powder X-ray diffraction (PXRD) was measured using a Shimadzu XRD 7000 (Cu Kα, λ= 1,5418 Å) diffractometer operating at 44 kV and 40 mA, with a scan rate of 2° mim^{-1}.

TEM. Transmission electron microscopy (TEM) images were undertaken using a field emission gun-type transmission electron microscope Jeol JEM 2100F, operating in the TEM mode with 200 kV accelerating voltage.

FTIR. Fourier-transform infrared spectroscopy (FTIR) was collected at a Cary 660 FTIR, in the Attenuated Total Reflectance (ATR) mode, within 4000 - 400 cm^{-1} and spectral increment of 1 cm^{-1}.

DRS. Diffuse reflectance spectroscopy (DRS) from 200 to 800 nm was measured in a Shimadzu 2450 spectrometer by using $BaSO_4$ as total reflectance standard, incidence angle of 0 °, and spectral increment of 1 nm.

PL. UC emission spectra were collected in a Fluorog-3 (Horiba FL3-22-iHR320) equipped with a double excitation (1200 groves/nm, blazed 330 nm), and a double emission (1200 groves/nm, blazed 500 nm) monochromator. The emission spectra were obtained using a 980 nm laser (Crystalaser DL980-1W-T0) with variable power densities as an excitation source. The emission spectra were corrected according to the photodetector spectral response. Time-resolved spectroscopy was obtained by using a CW diode pumped solid state (DPSS) laser with 980 nm output set at 1 W and a TTL trigger from the DeltaHub time-correlated single photon counting (TCSPC) electronic module, operating in the multi-channel scaling (MSC) system equipped in the Horiba FL3-22-iHR320 spectrofluorometer at 298 K.

Temperature-dependent PL. Emission spectra from 77 K to 373 K were measured in the previously mentioned Fluorolog 3 equipment. To control the temperature, a Linkam accessory (THMS600), with an optical fiber set (NA = 0.22 - Horiba-FL-3000/FM4-3000) was used. One of the key parameters for a luminescence temperature sensor is the relative thermal sensitivity (S_r) which provides information regarding the changes of Δ at each temperature by means of equation S1.

$$S_r(T) = \frac{1}{\Delta\,(T)} \left| \frac{\partial \Delta\,(T)}{\partial T} \right| \;(S1)$$

The temperature uncertainty or temperature resolution (δT) is also of paramount importance and it is expressed by equation S2. This parameter is related to the small temperature changes that can be detected in the measurements, being a combination of the nanoparticle emission features as well as the sensitivity of the photodetector used in the measurement. In Equation S3, I is the integrated intensity of the emission and δI is the error associated with the intensity of the measurement.

$$\delta T(T) = \frac{1}{S_r\,(T)} \left| \frac{\delta \Delta\,(T)}{\Delta T} \right| (S2)$$

$$\frac{\delta \Delta}{\Delta} = \sqrt{\left(\frac{\delta I_1}{I_1}\right)^2 + \left(\frac{\delta I_2}{I_2}\right)^2} \;(S3)$$

Supplementary note S2. FTIR Analyses
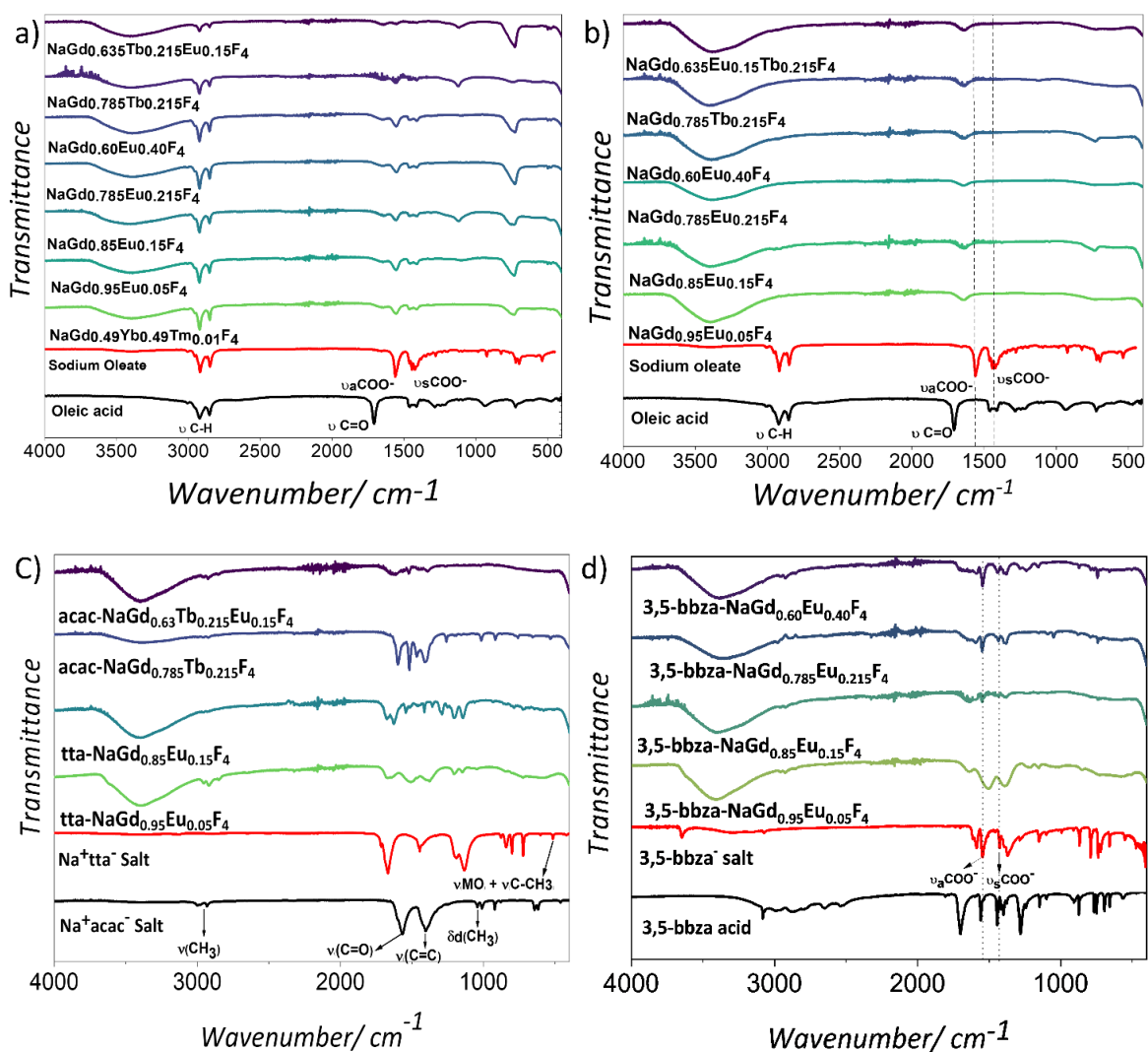
Figure S1. Fourier-transform infrared spectroscopy (FTIR) of (a) oleate-capped, (b) uncapped, (c) tta⁻- and acac⁻-functionalized, and (d) 3,5-bbza-functionalized nanoparticles. The respective ligand salt spectra of the acac⁻, tta⁻ and 3,5-bbza⁻ is also given for comparison .

Supplementary note S3. DRS Analyses

a)

$Absorbance$

NaGd$_{0.635}$Eu$_{0.15}$Tb$_{0.215}$F$_4$

NaGd$_{0.785}$Tb$_{0.215}$F$_4$

NaGd$_{0.60}$Eu$_{0.40}$F$_4$

NaGd$_{0.785}$Eu$_{0.215}$F$_4$

NaGd$_{0.85}$Eu$_{0.15}$F$_4$

NaGd$_{0.95}$Eu$_{0.05}$F$_4$

200 300 400 500 600 700 800

Wavelength / nm

b)

$Absorbance$

NaGd$_{0.635}$Eu$_{0.15}$Tb$_{0.215}$F$_4$

NaGd$_{0.785}$Tb$_{0.215}$F$_4$

NaGd$_{0.60}$Eu$_{0.40}$F$_4$

NaGd$_{0.785}$Eu$_{0.215}$F$_4$

NaGd$_{0.85}$Eu$_{0.15}$F$_4$

NaGd$_{0.95}$Eu$_{0.05}$F$_4$

200 300 400 500 600 700 800

Wavelength / nm
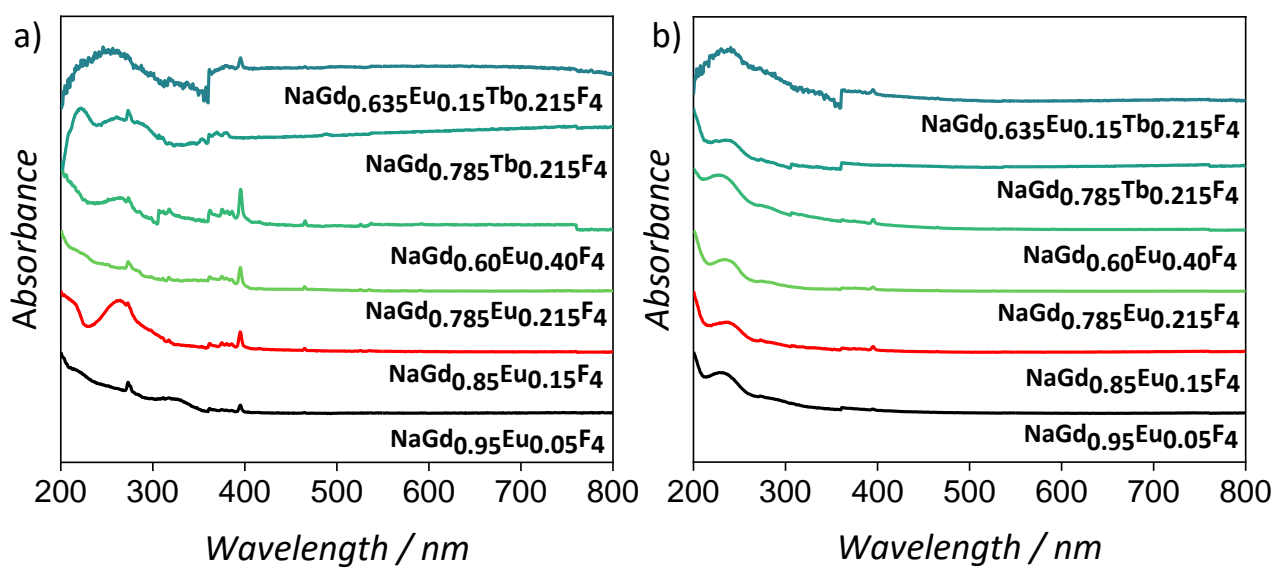
Figure S2. Diffuse reflectance spectra (DRS) of (a) oleate-capped nanoparticles (capped) and (b) oleate-free nanoparticles (uncapped).

Supplementary note S4. PL Analyses
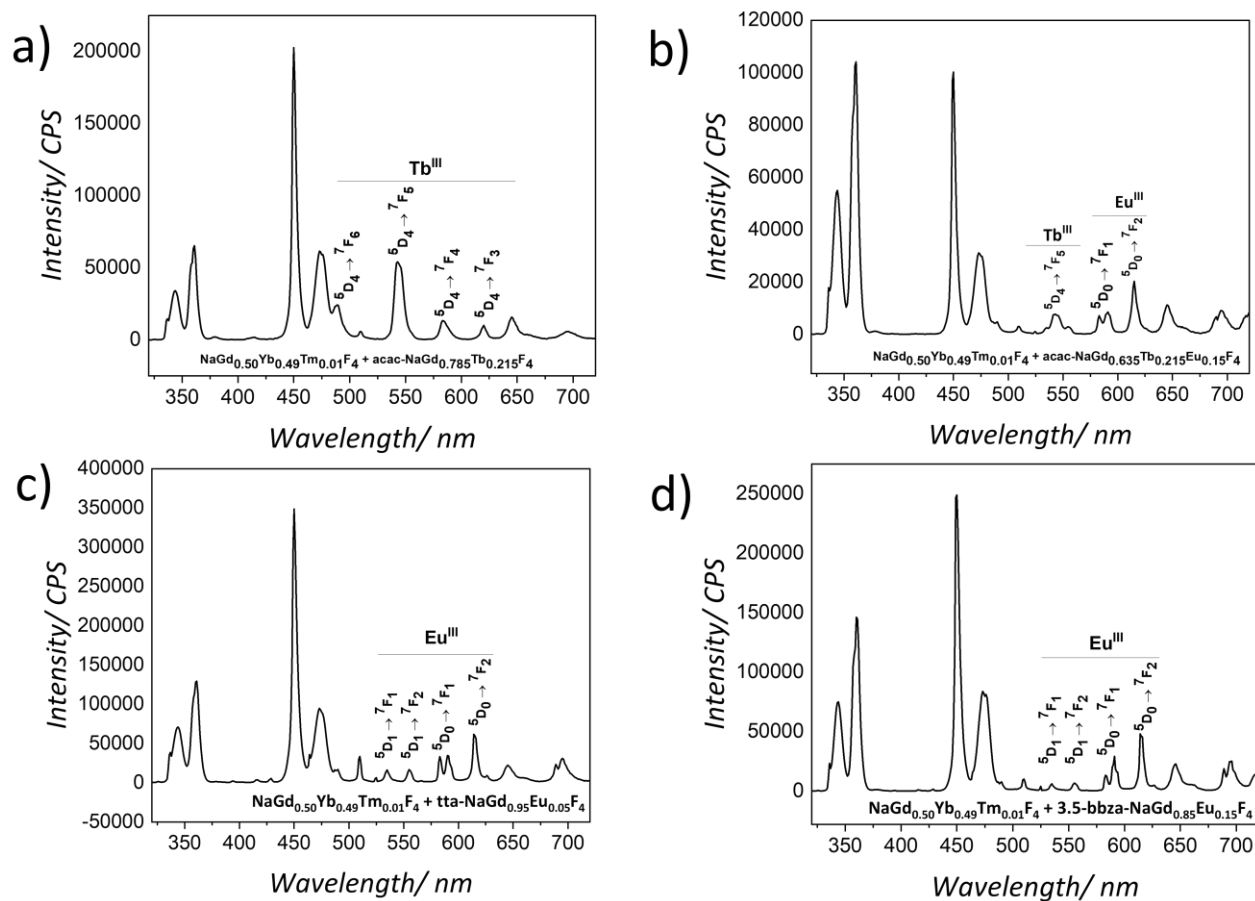
Figure S3. Emission spectra (λ_{exc} = 980 nm, 298 K) of acceptor NPs functionalized with (a) acac⁻, (b) acac⁻, (c) tta⁻, and (d) 3,5-bbza⁻ mixed with donor nanoparticle ($NaGd_{0.50}Yb_{0.49}Tm_{0.01}F_4$). The comparasion ensures that the nanoparticles functionalized with the acac⁻ present higher relative Eu^{III}/Tb^{III} emission intensities.
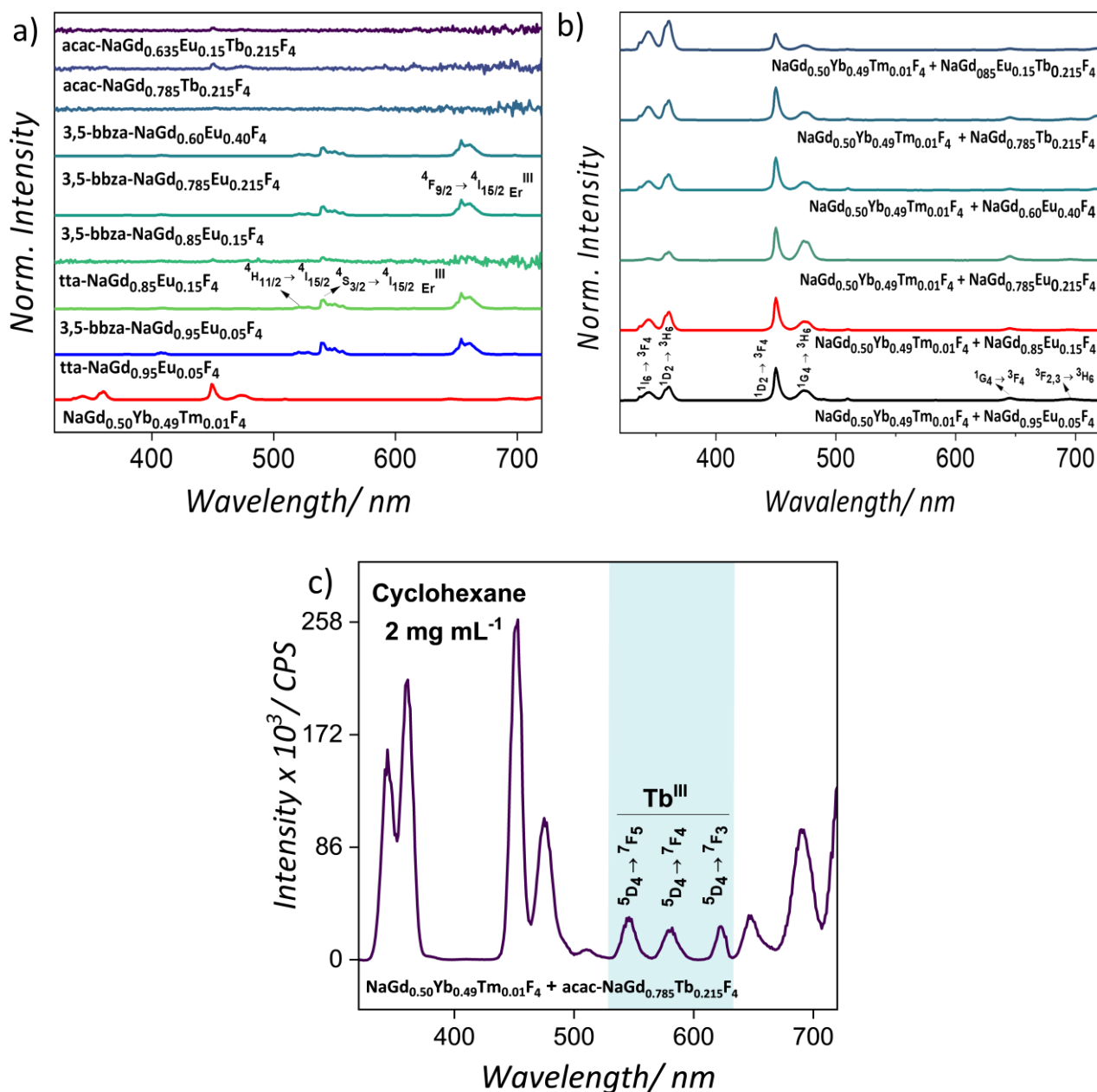
Figure S4. (a) Upconvesrion emission spectra (λ_{exc} 980 nm, 298 K, P= 40.4 W cm^{-2}) of the 3,5-bbza^{-}, acac^{-} or tta^{-}-functionalized nanoparticles without the donor nanoparticles. (b) Upconversion emission spectra (λ_{exc} 980 nm, 298 K, P= 40.4 W cm^{-2}) of the mixtures (1:1 w/w) containing the donor and the non-functionalized acceptor nanoparticles. In figure (b), only Er^{III} emissions are observed as a result of contaminant in the oxides used to prepare the precursors. (c) Upconversion emission spectra (λ_{exc} 980 nm, 298 K, P= 40.4 W cm^{-2}) of the acac^{-}-functionalized and donnor nanoparticle mixture (1:1 w/ w) dispersed in cyclohexane at concentration of 2 mg mL^{-1}.

Supplementary note S5. Power law analyses

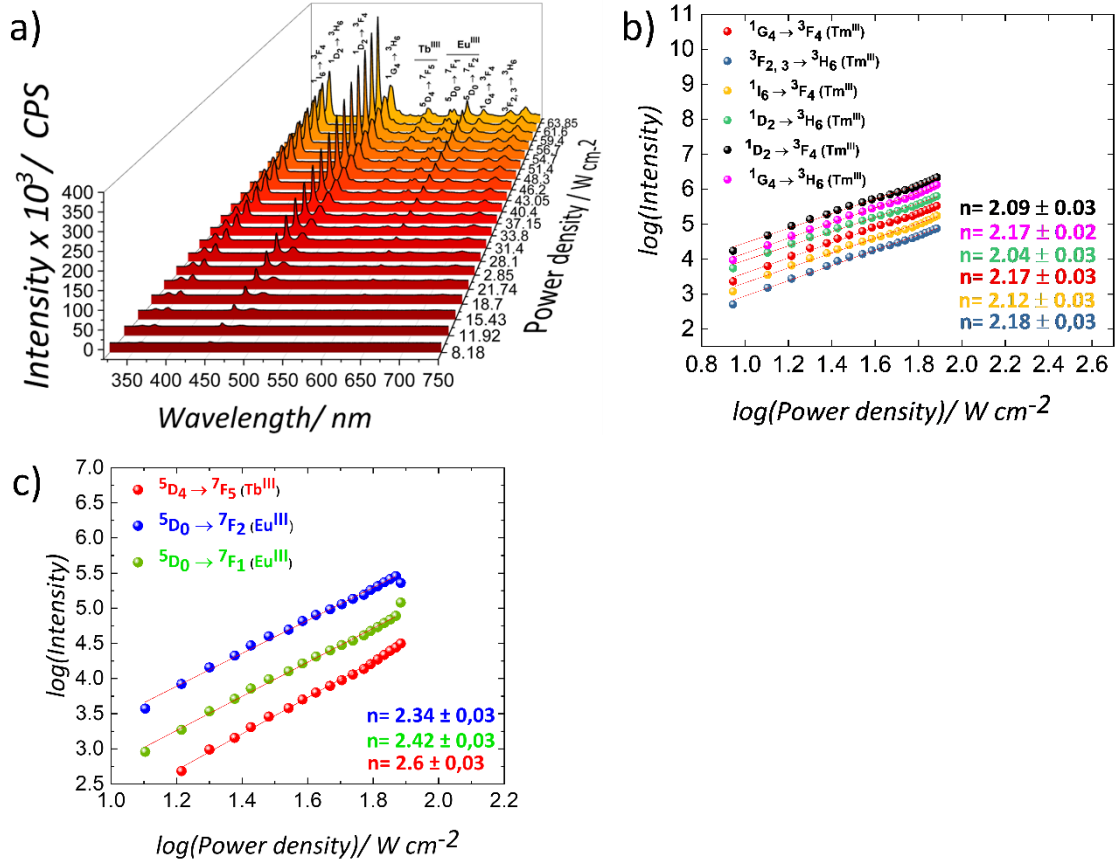**Figure S5.** (a) Upconversion emission spectra of the powder mixture: NaGd$_{0.50}$Yb$_{0.49}$Tm$_{0.01}$F$_4$ donor and acac$^-$-functionalized NaGd$_{0.635}$Eu$_{0.15}$Tb$_{0.21}$F$_4$ nanoparticle (298 K) at P$_{exc}$ ranging from 8.18 to 63.85 W cm^{-2} under 980 nm excitation. Dependence of the integrated emission intensities on the P_{exc} considering (b) Tm^{III} or (c) Eu^{III} and Tb^{III} emissions.

Supplementary note S6. PL lifetime

Table S1. Tm^{III} and Eu^{III} excited state lifetimes (λ_{exc}= 980 nm, 298 K) for the mixtures containing the 3,5-bbza$^-$-functionalized acceptor nanoparticles, compared to the donor nanoparticle without the acceptor nanoparticles.

States	YbTm/ ms	YbTm + Eu$_{0,05}$/ ms	YbTm + Eu$_{0,15}$/ ms	YbTm + Eu$_{0,215}$/ ms	YbTm + Eu$_{0,40}$/ ms
Tm^{III} $^1I_6 \rightarrow {}^3F_4$ (344 nm)	T$_1$: 0.069 ± 1x10^{-4} T$_2$: 0.589 ± 5.3 x 10^{-2}	T$_1$: 0.065 ± 1x10^{-4} T$_2$: 0.283 ± x 10^{-3}	T$_1$: 0.057 ± 1x10^{-4} T$_2$: 0.247 ± 5x10^{-3}	T$_1$: 0.078 ± 1x10^{-4} T$_2$: 0.604 ± 1.4x 10^{-2}	T$_1$: 0.073 ± 1x10^{-3} T$_2$: 0.356 ± 4x10^{-3}
Tm^{III} $^1D_2 \rightarrow {}^3H_6$ (361 nm)	T$_1$: 0.086 ± 2x10^{-4} T$_2$: 1.39 ± 0.503	T$_1$: 0.572 ± 6x10^{-3} T$_2$: 0.089 ± 8x10^{-5}	T$_1$: 0.072 ± 2x10^{-4} T$_2$: 0.285 ± 9x10^{-3}	T$_1$: 0.094 ± 1x10^{-4} T$_2$: 0.664 ± 1.2x 10^{-2}	T$_1$: 0.087 ± 1x10^{-3} T$_2$: 0.429 ± 4x10^{-3}
Tm^{III} $^1D_2 \rightarrow {}^3F_4$ (453 nm)	T$_1$: 0.085 ± 2x10^{-4} T$_2$: 1.36 ms ± 0.436	T$_1$: 0.081 ± 6x10^{-5} T$_2$: 0.532 ± x10^{-3}	T$_1$: 0.078 ± 1x10^{-4} T$_2$: 0.454 ± 2.4x10^{-2}	T$_1$: 0.09 ± 1x10^{-4} T$_2$: 0.565 ± 9x 10^{-3}	T$_1$: 0.088 ± 1x10^{-3} T$_2$: 0.604 ± 1.2x10^{-2}
Tm^{III} $^1G_4 \rightarrow {}^3H_6$ (475 nm)	T$_1$: 0.367 ± 2x10^{-4}	T$_1$: 0.432 ± 4x10^{-4}	T$_1$: 0.451 ± 3x10^{-3}	T$_1$: 0.434 ± 2x10^{-3}	T$_1$: 0.416 ± 2x10^{-3}
Eu^{III} $^5D_1 \rightarrow {}^7F_1$ (535 nm)	-	T$_1$: 0.363 ± 3x10^{-4} T$_2$: 1.9 ± 5x10^{-3}	T$_1$: 0.437 ± 3x10^{-3} T$_2$: 2.097± 4x10^{-3}	T$_1$: 0.128 ± 6x10^{-4} T$_2$: 0.56 ± 6x10^{-4}	T$_1$: 0.256 ± 3x10^{-4} T$_2$: 2.35 ± 6x10^{-3}
Eu^{III} $^5D_1 \rightarrow {}^7F_2$ (555 nm)	-	T$_1$: 0.324 ± 9x10^{-4} T$_2$: 1.88 ± 8x10^{-3}	T$_1$: 0.334 ± 2x10^{-3} T$_2$: 2.187 ± 3x10^{-3}	T$_1$: 0.14 ± 1x10^{-4} T$_2$: 0.652 ± 3x 10^{-3}	T$_1$: 0.238 ± 2x10^{-4} T$_2$: 2.14 ± 5x10^{-3}
Eu^{III} $^5D_0 \rightarrow {}^7F_1$ (591 nm)	-	T$_1$: 0.265 ± 2x10^{-3} T$_2$: 2.091 ± 2.4x10^{-2}	T$_1$: 0.417 ± 4x10^{-3} T$_2$: 2.368 ± 4x10^{-3}	T$_1$: 0.197 ± 4x10^{-4} T$_2$: 1 ± 3x10^{-3}	T$_1$: 0.212 ± 3x10^{-4} T$_2$: 2.414 ± 9x10^{-3}
Eu^{III} $^5D_0 \rightarrow {}^7F_2$ (615 nm)	-	T$_1$: 1.87 ± 5x10^{-3} T$_2$: 5.468 ± 6x10^{-3}	T$_1$: 5.547 ± 1.5x10^{-2}	T$_1$: 1.88 ± 1.1x10^{-2} T$_2$: 4.66 ± 1.5x10^{-2}	T$_1$: 1.554 ± 3x10^{-3} T$_2$: 4.01 ±4x10^{-3}
Tm^{III} $^1G_4 \rightarrow {}^3F_4$ (645 nm)	T$_1$: 0.385 ± 3x10^{-4}	T$_1$: 0.427 ± 2x10^{-3}	T$_1$: 0.176 ± 3x10^{-4} T$_2$: 0.471 ± 3x10^{-4}	T$_1$: 0.148 ± 7x10^{-4} T$_2$: 0.428 ± 9x10^{-4}	T$_1$: 0.18 ± 3x10^{-4} T$_2$: 0.470 ± 4x10^{-4}
Tm^{III} $^3F_{2, 3} \rightarrow {}^3H_6$ (695 nm)	T$_1$: 0.069 ± 1x10^{-4} T$_2$: 0.567 ± 3.5x10^{-2}	T$_1$: 0.142 ± 1x10^{-4} T$_2$: 4.173 ± 4.2x10^{-2}	T$_1$: 0.05 ± 1x10^{-4} T$_2$: 0.23 ± 3x10^{-3}	T$_1$: 0.05 ± 1x10^{-4} T$_2$: 0.233 ± 3x10^{-3}	T$_1$: 0.057 ± 1x10^{-4} T$_2$: 0.731 ± 2x10^{-3}

Table S2. Tm^{III} and Eu^{III} excited state lifetimes (λ_{exc}= 980 nm, 298 K) for the mixtures containing the tta$^-$-functionalized acceptor nanoparticles, compared to the donor nanoparticle without the acceptor nanoparticles.

States	YbTm/ ms	YbTm + Eu$_{0.05}$/ ms	YbTm + Eu$_{0.15}$/ ms
Tm^{III} $^1I_6 \rightarrow {}^3F_4$ (344 nm)	T$_1$: 0.069 ± 1x10^{-4} T$_2$: 0.589 ± 5.3 x 10^{-2}	T$_1$: 0.077 ± 1x10^{-4} T$_2$: 0.567 ± 8x10^{-3}	T$_1$: 0.071 ± 1x10^{-4} T$_2$: 0.389 ± 4x10^{-3}
Tm^{III} $^1D_2 \rightarrow {}^3H_6$ (361 nm)	T$_1$: 0.086 ± 2x10^{-4} T$_2$: 1.39 ± 0.503	T$_1$: 0.096 ± 1x10^{-4} T$_2$: 0.736 ± 6x10^{-3}	T$_1$: 0.088 ± 1x10^{-4} T$_2$: 0.596 ± 1x10^{-2}
Tm^{III} $^1D_2 \rightarrow {}^3F_4$ (453 nm)	T$_1$: 0.085 ± 2x10^{-4} T$_2$: 1.36 ± 0.436	T$_1$: 0.087 ± 9x10^{-5} T$_2$: 0.792 ± 6x10^{-3}	T$_1$: 0.08 ± 1x10^{-4} T$_2$: 0.744 ± 9x10^{-3}
Tm^{III} $^1G_4 \rightarrow {}^3H_6$ (475 nm)	T$_1$: 0.367 ± 2x10^{-4}	T$_1$: 0.462 ± 2x10^{-3}	T$_1$: 0.186 ± 1x10^{-3} T$_2$: 0.481 ± 2x10^{-3}
Eu^{III} $^5D_1 \rightarrow {}^7F_1$ (535 nm)	-	T$_1$: 1.931 ± 1.4x10^{-2}	T$_1$: 0.309 ± 1x10^{-3} T$_2$: 2.75 ± 1.4x10^{-2}
Eu^{III} $^5D_1 \rightarrow {}^7F_2$ (555 nm)	-	T$_1$: 0.533 ± 9x10^{-3} T$_2$: 2.35 ± 8.8x10^{-2}	T$_1$: 0.173 ± 1x10^{-3} T$_2$: 1.422 ± 8.8x10^{-2} T$_2$: 3.411 ± 2.41x10^{-1}
Eu^{III} $^5D_0 \rightarrow {}^7F_1$ (591 nm)	-	T$_1$: 4.48 ± 1.19x10^{-1} T$_2$: 0.134 ± 1x10^{-3} T$_2$: 1.079 ± 1.5x10^{-2}	T$_1$: 0.353 ± 3x10^{-3} T$_2$: 3.513 ± 9.5x10^{-2}
Eu^{III} $^5D_0 \rightarrow {}^7F_2$ (615 nm)	-	T$_1$: 8.18 ± 2.4x10^{-2}	T$_1$: 7.13 ± 2.8x10^{-2}
Tm^{III} $^1G_4 \rightarrow {}^3F_4$ (645 nm)	T$_1$: 0.385 ± 3x10^{-4}	T$_1$: 0.46 ± 2x10^{-3}	T$_1$ 0.16 ± 3x10^{-4} T$_2$: 0.471 ± 3x10^{-4}
Tm^{III} $^3F_{2.3} \rightarrow {}^3H_6$ (695 nm)	T$_1$: 0.069 ± 1x10^{-4} T$_2$: 0.567 ± 3.5x10^{-2}	T$_1$ 0.071 ± 9x10^{-5} T$_2$: 0.458 ± 7x10^{-3}	T$_1$ 0.06 ± 9x10^{-5} T$_2$: 0.329 ± 2x10^{-3}

Table S3. Tm^{III}, Eu^{III} and Tb^{III} excited state lifetimes (λ_{exc}= 980 nm, 298 K) for the mixtures containing the acac⁻-functionalized acceptor nanoparticles, compared to the donor nanoparticle without the acceptor nanoparticles.

States	YbTm/ ms	YbTm + $Eu_{0,15}Tb_{0,215}$/ ms	YbTm + $Tb_{0,215}$/ ms
Tm^{III} $^1I_6 \rightarrow {}^3F_4$ (344 nm)	T_1: 0.069 ± 1x10^{-4} T_2: 0.589 ± 5.3 x 10^{-2}	T_1: 0.069 ± 9x10^{-5} T_2: 0.305 ± 2x10^{-3}	T_1: 0.082 ± 1x10^{-4} T_2: 0.56 ± 1.1x10^{-2}
Tm^{III} $^1D_2 \rightarrow {}^3H_6$ (361 nm)	T_1: 0.086 ± 2x10^{-4} T_2: 1.39 ± 0.503	T_1: 0.084 ± 1x10^{-4} T_2: 0.367 ± 3x10^{-3}	T_1: 0.098 ± 1x10^{-4} T_2: 0.602 ± 9x10^{-3}
Tm^{III} $^1D_2 \rightarrow {}^3F_4$ (453 nm)	T_1: 0.085 ± 2x10^{-4} T_2: 1.36 ms ± 0.436	T_1: 0.081 ± 1x10^{-4} T_2: 0.346 ± 3x10^{-3}	T_1: 0.094 ± 1x10^{-4} T_2: 0.492 ± 6x10^{-3}
Tm^{III} $^1G_4 \rightarrow {}^3H_6$ (475 nm)	T_1: 0.367 ± 2x10^{-4}	T_1: 0.528 ± 3x10^{-3}	T_1: 0.468 ± 2x10^{-3}
Tb^{III} $^5D_4 \rightarrow {}^7F_6$ (488 nm)	-	-	T_1: 5.03 ± 1.4x10^{-2}
Tb^{III} $^5D_4 \rightarrow {}^7F_5$ (544 nm)	-	T_1: 1.34 ± 2x10^{-3} T_2: 3.43 ± 2x10^{-3}	T_1: 4.89 ± 1.7x10^{-2}
Tb^{III} $^5D_4 \rightarrow {}^7F_4$ (581 nm)	-	-	T_1: 5.03 ± 1.4x10^{-2}
Tb^{III} $^5D_4 \rightarrow {}^7F_3$ (622 nm)	-	-	T_1: 5.18 ± 1.5x10^{-2}
Eu^{III} $^5D_0 \rightarrow {}^7F_1$ (591 nm)	-	T_1: 3.09 ± 1x10^{-2} T_2: 0.615 ± 4x10^{-3}	-
Eu^{III} $^5D_0 \rightarrow {}^7F_2$ (615 nm)	-	T_1: 1.76 ± 3x10^{-3} T_2: 4.6 ± 4x10^{-3}	-
Tm^{III} $^1G_4 \rightarrow {}^3F_4$ (645 nm)	T_1: 0.385 ± 3x10^{-4}	T_1: 0.487 ± 2x10^{-3}	T_1: 0.193 ± 1x10^{-3} T_2: 0.515 ± 2x10^{-3}
Tm^{III} $^3F_{2,3} \rightarrow {}^3H_6$ (695 nm)	T_1: 0.069 ± 1x10^{-4} T_2: 0.567 ± 3.5x10^{-2}	T_1: 1.15 ± 5x10^{-3} T_2: 4.12 ± 5x10^{-3}	T_1: 0.079 ± 1x10^{-4} T_2: 0.524 ± 7x10^{-3}

Table S4. Tm^{III} excited state lifetimes (λ_{exc}= 980 nm, 298 K) for the mixtures containing the donnor nanoparticle and the [Gd(3,5-bbza)₃] complex.

| states	YbTm/ ms	YbTm + Gd(bbza)₃/ ms
Tm^{III} $^1I_6 \rightarrow {}^3F_4$ (343 nm)	T_1: 0.084 ± 2x10^{-3} T_2: 0.515 ± 3.7x10^{-2}	T_1: 0.065 ± 5x10^{-4} T_2: 0.377 ± 1.4x10^{-2}
Tm^{III} $^1D_2 \rightarrow {}^3H_6$ (360 nm)	T_1: 0.128 ± 2.8x10^{-3} T_2: 0.920 ± 3.6x10^{-2}	T_1: 0.080 ± 5.7x10^{-4} T_2: 0.445 ± 1.7x10^{-2}
Tm^{III} $^1D_2 \rightarrow {}^3F_4$ (450 nm)	T_1: 0.126 ± 2.6x10^{-3} T_2: 1.01 ± 1.6x10^{-2}	T_1: 0.077 ± 2.8x10^{-3} T_2: 0.427 ± 9x10^{-2}
Tm^{III} $^1G_4 \rightarrow {}^3H_6$ (473 nm)	T_1: 0.265 ± 1.1x10^{-2} T_2: 0.650 ± 1.5x10^{-2}	T_1: 0.16 ± 5x10^{-3} T_2: 0.373 ± 2.5x10^{-3}
Tm^{III} $^1G_4 \rightarrow {}^3F_4$ (645 nm)	T_1: 0.245 ± 6.6x10^{-3} T_2: 0.631 ± 1x10^{-2}	T_1: 0.150 ± 7.9x10^{-3} T_2: 0.363 ± 5.1x10^{-3}
Tm^{III} $^3F_{2,3} \rightarrow {}^3H_6$ (689 nm)	T_1: 0.069 ± 1x10^{-4} T_2: 0.567 ± 3.5x10^{-2}	T_1: 0.054 ± 1x10^{-3} T_2: 0.301 ± 5.1x10^{-3}
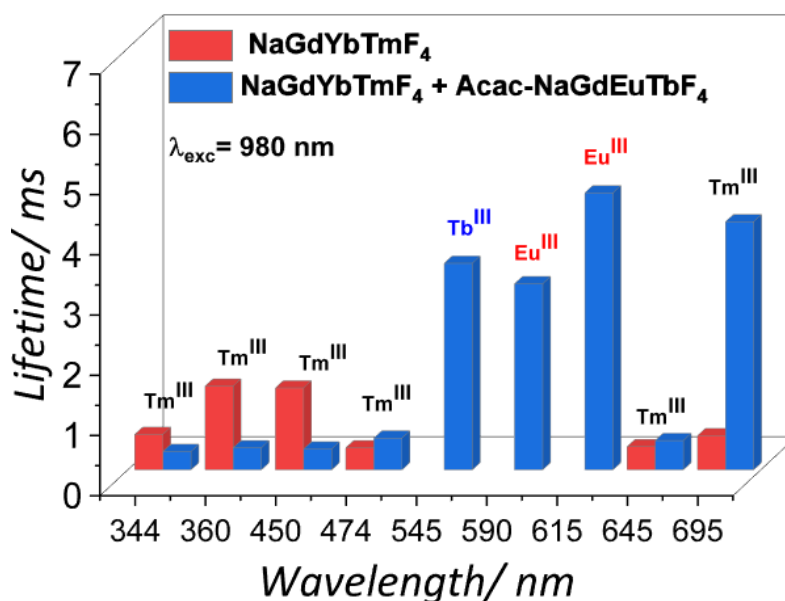
Figure S6. Comparison of the Tm^{III} excited state lifetimes in the isolated $NaGd_{0.50}Yb_{0.49}Tm_{0.01}F_4$ donnor nanoparticle (red bar) and in the $NaGd_{0.50}Yb_{0.49}Tm_{0.01}F_4$ + acac-$NaGd_{0.635}Eu_{0.15}Tb_{0.215}F_4$ mixture (blue bar).
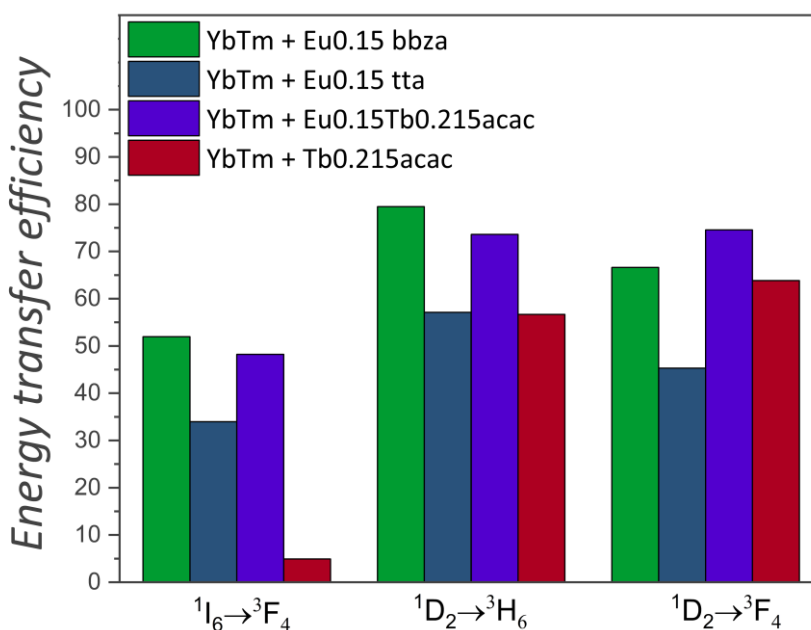

Figure S7. Tm^{III}-to-Ln^{III} (Ln = Eu and/or Tb) energy transfer efficiencies calculated from eqn S4, where τ_1 is the Tm^{III} emitting state lifetime in the presence of the acceptor nanoparticle and τ_{10} is the Tm^{III} emitting state lifetime without the acceptor nanoparticle.

$$\eta = 1 - \frac{\tau_1}{\tau_{10}} \ (S4)$$

Supplementary references

1 E. M. Rodrigues, D. A. Gálico, I. O. Mazali and F. A. Sigoli, *Methods Appl. Fluoresc.*, 2017, **5**, 024012.

2 N. Liu, N. Gobeil, P. Evers, I. Gessner, E. M. Rodrigues and E. Hemmer, *Dalton Trans.*, 2020, **49**, 16204–16216.